water

MDPI

Article

Vulnerability Assessment and Future Prediction of Urban Waterlogging—A Case Study of Fuzhou

Xuerao Wang [1,2], Zhiming Zhang [1,2,*], Wenhan Hu [1,2], Xin Zhao [3], Xiaotian Qi [4] and Ran Cai [5]

[1] School of Environmental and Energy Engineering, Beijing University of Civil Engineering and Architecture, Beijing 100044, China; alien0103@163.com (X.W.); huwenhan1998@163.com (W.H.)
[2] Beijing Climate Change Response Research and Education Center, Beijing University of Civil Engineering and Architecture, Beijing 100044, China
[3] North China Municipal Engineering Design & Research Institute Co., Ltd., Tianjin 300074, China; zx175246@163.com
[4] School of Environmental Science and Engineering, Tianjin University, Tianjin 300072, China; qixiaotian1997@163.com
[5] Beijing Capital Ecological Protection Group, Beijing 100044, China; cairan@capitalwater.cn
* Correspondence: zhangzhiming@bucea.edu.cn; Tel.: +86-010-6832-4119

Abstract: Evaluating waterlogging vulnerability and analyzing its characteristics and future trends can provide scientific support for urban disaster prevention and reduction. For this study, taking Fuzhou as an example, an urban waterlogging vulnerability assessment system was constructed from the three dimensions of exposure, sensitivity, and adaptive capacity. The entropy method was used to evaluate urban waterlogging vulnerability in Fuzhou during 2014–2020. The use of CA–Markov to predict waterlogging vulnerability in 2023, 2026, and 2029 in Fuzhou is an important innovation reported in this paper. Study results showed that: (1) Vulnerability to waterlogging in Fuzhou follows a gradually decreasing "center-southeast" distribution pattern, with Level 5 areas mainly located in Cangshan District, Gulou District, and Taijiang District. (2) Changes in waterlogging vulnerability in Fuzhou from 2014 to 2020 can be divided into five change modes, with changing areas, mainly of the late-change type, accounting for 14.13% of the total area. (3) Prediction accuracy verification shows that the CA–Markov model is suitable for predicting waterlogging vulnerability in Fuzhou with high accuracy and a kappa coefficient of 0.9079. (4) From 2020 to 2029, the vulnerability level of the eastern coastal region of Fuzhou is expected to generally increase, and the vulnerability degree will continue to deteriorate. The proportion of Level 5 vulnerable areas will increase by 4.5%, and the growth rate will increase faster and faster with the passage of time.

Keywords: waterlogging vulnerability; Fuzhou; CA–Markov model; dynamic change; index system

Citation: Wang, X.; Zhang, Z.; Hu, W.; Zhao, X.; Qi, X.; Cai, R. Vulnerability Assessment and Future Prediction of Urban Waterlogging—A Case Study of Fuzhou. *Water* **2023**, *15*, 4025. https://doi.org/10.3390/w15224025

Academic Editor: Elias Dimitriou

Received: 24 September 2023
Revised: 3 November 2023
Accepted: 16 November 2023
Published: 20 November 2023

1. Introduction

Urban waterlogging vulnerability indicates the degree of damage that the socioeconomic activities of a city may suffer under the disturbance or pressure of waterlogging, i.e., the nature of the region's vulnerability to injury and loss when facing waterlogging. Because reducing vulnerability to waterlogging effectively reduces disaster risk and improves resilience, it has become a critical issue in urban development and water hazard research [1].

The main methods for assessing vulnerability to waterlogging are the indicator system method and the vulnerability curve method [2,3]. The vulnerability curve method, also known as the disaster loss curve method, assesses vulnerability by constructing a function between different hazard intensities and losses of disaster-bearing bodies. Accurate and credible results may be obtained using this method [4]. The data used for curve fitting are mainly historical disaster data, field research data, insurance data, etc. The HAZUS-MH (Hazard United States—Multi-Hazard) [5] software developed by the Federal Emergency

Management Agency of the United States, and the EMA-DLA (Emergency Management Australia—Disaster Loss Assessment) [6] software developed by the Australian Emergency Management Agency are both widely used internationally. The indicator system method selects assessment indicators and constructs vulnerability indices according to the characteristics of the study area and hazard features, and can thus assess vulnerability to waterlogging more comprehensively and accurately. The indicator system method is less dependent on historical disaster data than the vulnerability curve method. It has a broader scope of application, from large-scale international plans to small-scale community vulnerability studies. For example, Li et al. [7] conducted a waterlogging vulnerability assessment of old neighborhoods and found that waterlogging vulnerability was higher in neighborhoods with longer construction times and a more backward living infrastructure. Zheng et al. [8] comprehensively analyzed the waterlogging vulnerability of 17 municipal administrations in Hubei Province and found that waterlogging vulnerability was higher in municipal administrations located in the southeastern region. In addition, the indicator system method can identify the factors affecting vulnerability, so that human beings can make corresponding countermeasures in a targeted manner. Helderop et al. [9] showed that population growth and urban development lead to an increase in vulnerability to urban flooding. Using the hierarchical analysis method, Huang et al. [10] found that water surface area and drainage network density are the key factors affecting vulnerability to urban flooding, and Christian et al. [11] found that the education level of residents and gender differences significantly affect vulnerability to regional flooding.

With in-depth studies of waterlogging vulnerability, scholars have found that the time scale determines the degree of damage and impact caused by storm waterlogging disasters in a city [12], and that vulnerability to waterlogging in the same area tends to change due to different time scales. However, previous studies have mainly focused on vulnerability evaluation in present-day urban situations; there have been fewer studies on the changing status of vulnerability and predictions of future development. Scientific prediction can help decision-makers understand the future development of waterlogging vulnerability so that existing measures may be adjusted, or new measures formulated, to mitigate risk and reduce the loss in time. Some studies have predicted vulnerability using specific mathematical and theoretical models, but their prediction accuracy has been low. For example, Yi et al. [13] used the vulnerability index as the dependent variable and the influence factor as the independent variable to build a neural network model to assess and predict vulnerability in Urumqi city. However, the average error reached 14.64%. With the rapid development of GIS, RS, and big data technologies, the accuracy of data acquisition is growing higher and higher, and how to improve the accuracy of vulnerability prediction has become the focus of research by scholars today.

The CA–Markov model is a lattice dynamics model which combines the ability of the CA (cellular automata) model to predict the evolution of spatial patterns with the ability of the Markov model to extrapolate time series. It has been widely used for predicting the evolution of land use and vegetation cover [14,15]. In addition, some scholars have gradually introduced the CA–Markov model into their future-prediction research relating to vulnerable areas. For example, Yao et al. [16] used the CA–Markov model to simulate and predict the development of ecological vulnerability in the middle and upper Yalong River basin, and thereby revealed a pattern of dynamic changes in the future development of ecological vulnerability in the region. Marzieh et al. [17] used CA–Markov to predict drought vulnerability in southwest Iran and found that the predicted drought map was highly consistent with the observed drought map. It can be seen that the CA–Markov model has high prediction accuracy and adaptability, but it has been less widely used in studies in waterlogging vulnerability.

Therefore, it is necessary to address the issue of insufficient exploration in existing research on predicting future vulnerability to waterlogging. As a typical representative of coastal cities in the south of China, Fuzhou City is a disaster area that is greatly affected by typhoons and rainstorms on a national scale. Meanwhile, with the accelerated progress of

urbanization in Fuzhou, the proportion of impermeable surface area is increasing, so that surface runoff volume is also increasing, and flooding disasters occur frequently. Therefore, conducting an urban flood vulnerability assessment in Fuzhou may provide support for flood disaster management, and for disaster prevention and mitigation, in the city, as well as providing some reference for flood vulnerability assessments in other coastal cities. For the study described in this paper, we constructed a vulnerability assessment system for urban waterlogging in Fuzhou based on the VSD model framework to assess the vulnerability of Fuzhou and predict the future development of vulnerability using the CA–Markov model, to provide support for waterlogging disaster management, and for disaster prevention and mitigation, in Fuzhou.

2. Materials and Methods

2.1. Study Area

Fuzhou is located on the southeast coast of China, in the eastern part of Fujian Province, downstream of the Min River by the sea. The city has 13 counties and districts under its jurisdiction, as shown in Figure 1. As a typical representative of China's eastern coastal cities, it is a disaster area which is greatly affected by typhoons and rainstorms nationwide. Fuzhou experiences many days of rainstorms and high-intensity rain. At the same time, with the accelerated progress of urbanization in Fuzhou, the proportion of impervious surface area is increasing, so that surface runoff is also increasing, and waterlogging disasters occur frequently.

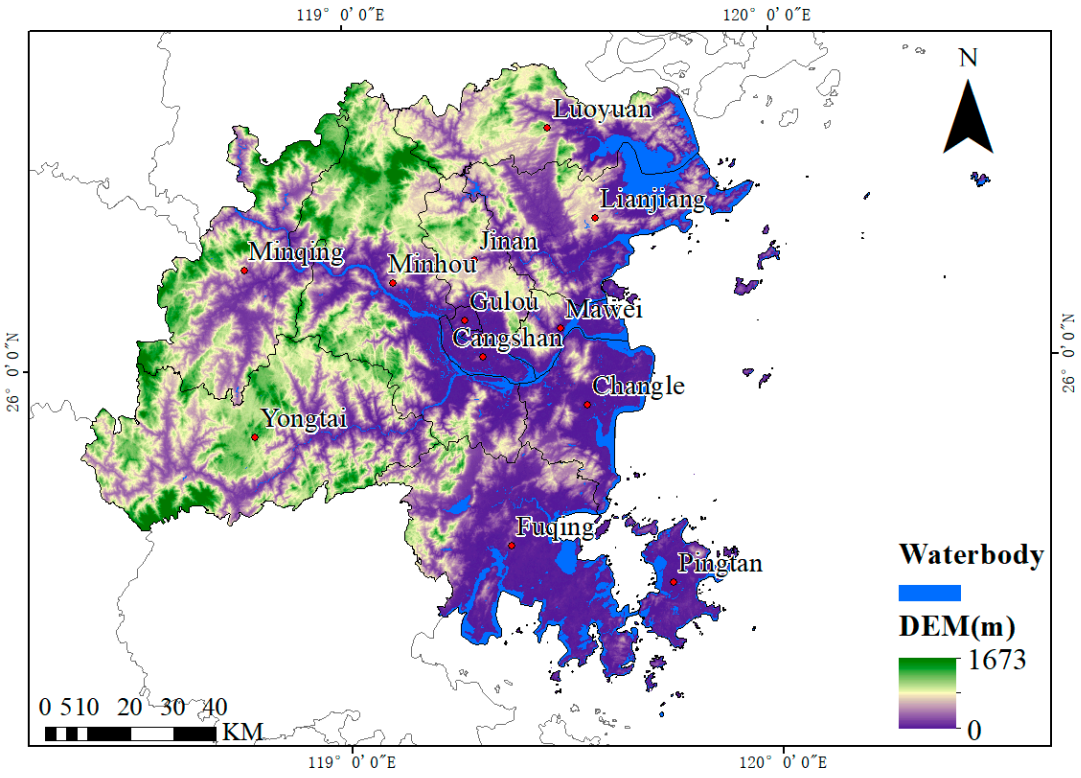

Figure 1. Administrative division of Fuzhou.

2.2. Data Source

The data types and sources used in this study are shown in Table 1. Because different data sources exist, there are also gaps in the coordinate system and resolution. All data coordinate systems are projected as WGS_1984_UTM_ZONE_50N, with grid resolution resampled to 100 m by the nearest neighbor technique, to prevent mistakes in overlay computations.

Table 1. Names and sources of study area base data.

Data Type	Data Name	Data Source
Meteorological data	Daily meteorological dataset of basic meteorological elements of China National Surface Weather Station (V3.0)	Data Center for Resources and Environmental Sciences, Chinese Academy of Sciences (https://www.resdc.cn (accessed on 1 September 2022))
Geographic information data	Digital elevation model (30 m resolution)	Geospatial data cloud (https://www.gscloud.cn (accessed on 1 September 2022))
	Night-lighting data (1000 m resolution)	National Centers for Environmental Information (NCEI) (https://www.ncei.noaa.gov (accessed on 1 September 2022))
	Normalized difference vegetation index spatial distribution dataset in China (100 m resolution)	Data Center for Resources and Environmental Sciences, Chinese Academy of Sciences (https://www.resdc.cn (accessed on 1 September 2022))
	Road network, building, water system vector data	OpenStreetMap (https://www.openstreetmap.org (accessed on 1 September 2022))
	Land use data (10 m resolution)	European Space Agency (www.esa.int (accessed on 1 September 2022))
	Population distribution data (100 m resolution)	WorldPop (https://www.worldpop.org (accessed on 1 September 2022))
Socioeconomic data	Education, medical, disaster prevention, and control data	Fuzhou Statistical Yearbook
	Emergency shelter data	Fuzhou Municipal People's Government

2.3. Technical Process

A flowchart of the process used for the present study is shown in Figure 2.

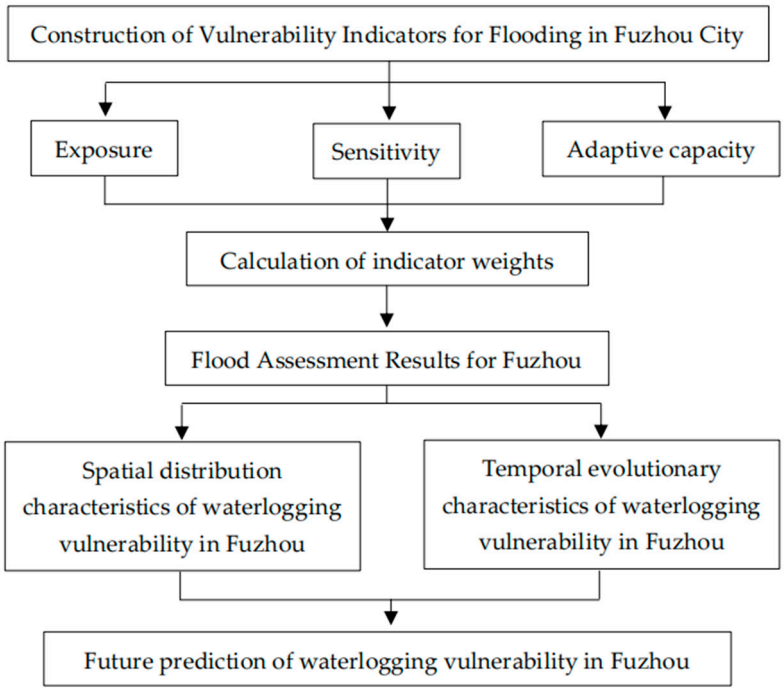

Figure 2. Flowchart of the study process.

2.4. Index System Construction

For this study, we established an index system based on the VSD model, which has a wider scope of application than other models [18]. Exposure refers to the extent to which a city is adversely affected by external pressure or stress, including the influence range

of the causal factors and the spatial location distribution of the disaster-bearing body. Sensitivity refers to the degree of response of urban disaster-bearing bodies to waterlogging disturbances; this is determined by the nature of the disaster-bearing bodies themselves, including their natural and social characteristics. Adaptive capacity refers to the effective measures taken by humans in response to waterlogging hazards.

Based on the theory of waterlogging vulnerability, and the current situation with regard to waterlogging disasters in Fuzhou, 20 evaluation indicators were selected to build an indicator system for assessment of waterlogging vulnerability in Fuzhou, as shown in Table 2. The entropy method was used to calculate the index's weight and thus avoid the influence of human factor of subjective method.

Table 2. Urban waterlogging vulnerability assessment index system for Fuzhou.

Guideline Layer	Indicator Layer	Indicator Properties	Indicator Meaning
Exposure	Total annual rainfall	Positive	The annual rainfall totals represent the overall spatial distribution differences of rainfall in the region. The higher the rainfall, the higher the risk of waterlogging and the higher the vulnerability of the area [19].
	Number of annual rainstorms	Positive	The sum of the annual number of heavy rainfall events (daily rainfall $\geq$ 50 mm or rainfall $\geq$ 30 mm in 12 h) in Fuzhou.
	Annual storm peak	Positive	The peak amount of daily rainstorms in a year. The city's waterlogging volume is also greatest during the peak period, and the city's traffic congestion and drainage network operation are related to this indicator [20].
	Population density	Positive	The density of the population within the area. The body most directly affected by urban waterlogging is the urban population.
	Road network density	Positive	Reflection of the traffic operation in the region, expressed by the length of the road network per unit area.
	Building density	Positive	Urban buildings are the main disaster-bearers of internal waterlogging. The greater the building density, the greater the economic loss, and the normalized difference build-up index can reflect the building density more accurately.
Sensitivity	Night lighting	Positive	Indicators reflecting human activity and economic activity [21,22].
	Soil water retention	Negative	Reactive surface runoff. Surface runoff during rainfall is one of the important factors contributing to the risk of waterlogging, and surface runoff is related to soil water-holding capacity [23].
	Distance from the water system	Negative	Heavy rainfall events often cause urban waterlogging. When the rainfall exceeds the storage capacity of water systems, rivers tend to spill out, thus becoming a new source of disaster.
	Slope	Negative	Reflection of the degree of surface tilt. The slope of the ground can accelerate the water catchment to form groundwater, and when the drainage is poor, it develops into internal waterlogging.
	Normalized difference vegetation index	Negative	Reflection of the vegetation cover of the region. Vegetation can effectively reduce surface runoff.
	Topographic wetness index	Positive	The topographic wetness index can reflect the influence of topography on the area of catchment production. The higher the topographic wetness index, the larger the catchment area on the area's slope, or the steeper the hydraulic gradient, the more likely the production of runoff [24–26].

Table 2. *Cont.*

Guideline Layer	Indicator Layer	Indicator Properties	Indicator Meaning
	Topographic position index	Negative	Reflection of the effect of local elevation on runoff, defined as the difference between the center-point elevation and the mean elevation in the center-point domain [27].
	Contagion index	Positive	Landscape sprawl is positively correlated with the degree of regional inundation, so the greater the landscape sprawl, the higher the inundation vulnerability [28].
	Shannon's diversity index	Negative	The diversity of the landscape is negatively correlated with the degree of regional waterlogging, i.e., the more complex the overall urban landscape, and the richer its composition types, the less likely it is to cause regional waterlogging hazards [28].
Adaptive capacity	Education level	Negative	The higher the education level of residents, the better their ability to recognize and judge risks and their ability to cope with them. Regional education expenditure indicates the education level of residents [29].
	Medical level	Negative	The regional medical level is related to the health of citizens and the level of health services. It is an important guarantee for the sustainable development of human society [30,31]. The medical expenditure of each county in Fuzhou City indicates the regional medical level.
	Disaster prevention and control capacity	Negative	Reflection of the government's ability to both prevent and manage disasters, and rebuild after them, using expenditures on disaster prevention and emergency management.
	Emergency evacuation distance	Positive	Reflection of the ability of the region to respond to public emergencies [22]. The distance from the center of each grid to the initial point is calculated using the emergency shelter as the initial point.
	Drainage pipe network design standards	Negative	The design standard of drainage networks is an important factor affecting urban waterlogging. When the intensity of rainfall exceeds the urban drainage network design standard, the groundwater cannot be removed in time, thus causing waterlogging in local areas. This study refers to the requirements of the design return period of rainwater drains in the Outdoor Drainage Design Standard GB50014–2021 [32], and the scope of the central city area as stipulated in the Fuzhou City Master Plan (2011–2020), and assigns values according to the importance of the geographical location of different areas.

2.5. Waterlogging Vulnerability Index and Classification

Waterlogging vulnerability may calculated based on indicator weights using the following formula:

$$WVI = E + S - A = \sum_{i=1}^{n} \delta_{ei} X_{ei} + \sum_{i=1}^{n} \delta_{si} X_{si} - \sum_{i=1}^{n} \delta_{ai} X_{ai} \quad (1)$$

where WVI is waterlogging vulnerability; E is exposure; S is sensitivity; A is adaptive capacity; δ_{ei}, δ_{si}, and δ_{ai} are the weights of the indicators of exposure, sensitivity, and adaptive capacity, respectively; X_{ei}, X_{si}, and X_{ai} are exposure, sensitivity, and adaptive capacity values, respectively; and n is the number of indicators in each dimensional layer.

The WVI values for each year were graded by the "natural intermittent point grading method", and the upper and lower thresholds of each grade were found. Finally, an average value of thresholds of the same grade was taken as the final criterion for data classification. The WVI was classified into Level 1, Level 2, Level 3, Level 4, and Level 5; the higher the level, the more severe the vulnerability.

2.6. CA–Markov Model

Cellular automata comprise cells, cell states, cell space, a cell neighborhood, and cell rules [33]. The cell is the most basic unit of cellular automata, and its composition differs according to different models. The cell state is the state to which the cell belongs at a given time. Cell space is an expanse of space in which cells are located, and which can be divided into one dimension, two dimensions, or multiple dimensions, with two-dimensional cellular automata being widely used. Cell neighborhood refers to the geometric position and state of a cell adjacent to it. Cell rules are the transition rules that determine the state of the cell at the next moment. In this study, two-dimensional cell space is used, and the grid of vulnerability data for Fuzhou is taken as the cell. Each cell has a certain area and a certain coordinate. The cellular state is divided into five categories: Level 1, Level 2, Level 3, Level 4, and Level 5. A 5×5 filter is selected to define the cell neighborhood; this means that 24 cells around the filter affect the properties of the cell. Markov chains are used as cell conversion rules.

The Markov model is also known as a Markov chain. It can use the empirical transition probability of the existing discrete state of the system to simulate and predict future development [34]. Markov chains have "memoryless" properties, meaning that the probability distribution of the system state at time $t + 1$ is only related to the state at time t, and is independent of the state before time t. It can be expressed by the formulas below [35]:

$$S(t+1) = P_{ij} \times S(t) \tag{2}$$

$$P_{ij} = \begin{pmatrix} P_{11} & \cdots & P_{1n} \\ \vdots & \ddots & \vdots \\ P_{n1} & \cdots & P_{nn} \end{pmatrix} \tag{3}$$

where $S(t)$ and $S(t+1)$ denote the states of the system at moments t and $t+1$, respectively; P_{ij} is the state transfer matrix; i and j represent the two initial end-time points; and n is each vulnerability level in the study area.

The CA–Markov model combines the ability of cellular automata to simulate the spatial variability of the system with the advantage of Markov long-term prediction. For this reason, the CA–Markov model was used in this study to carry out simulation and prediction of urban waterlogging vulnerability in Fuzhou.

IDRISI is a software that perfectly combines GIS and image-processing functions. IDRISI17.0 software was used to complete the CA–Markov simulation prediction. The key steps of the process used in the present study were as follows:

(1) Data format conversion and reclassification: the waterlogging vulnerability assessment results for Fuzhou were converted into the raster data format supported by IDRISI and reclassified in IDRISI according to the vulnerability classification criteria.

(2) Generating the transfer matrix: the Markov model was used to generate the transfer matrix of waterlogging vulnerability states.

(3) Logistic was applied to analyze each flooding vulnerability level that might occur in each raster, and the spatial distribution probability maps of each flooding vulnerability level were obtained. The suitability maps for each individual flooding vulnerability level were superimposed using a collection editor in IDRISI software, and the suitability atlas was obtained as a transformation rule for CA–Markov, which was used as the basis for the prediction.

(4) Defining the cell neighborhood: an appropriate filter was selected to define the cell neighborhood.

(5) Determining the iteration coefficient: Because the data used had a time interval of 3 years, the time interval for the number of cycles was also set to 3 years; the iteration coefficient was therefore taken to be 3. The equivalence coefficient was determined to be as 0.15 [36] by referring to the corresponding literature to complete the simulation prediction of waterlogging vulnerability in Fuzhou.

2.7. Accuracy Check

The kappa coefficient is a measure of accuracy. The CROSSTAB module in IDRISI17.0 software was used to calculate the kappa coefficient to verify the accuracy of the CA–Markov model simulation results. The calculation equation is as follows [37]:

$$k = \frac{P_o - P_e}{1 - P_e} \tag{4}$$

where P_o is the proportion of correctly predicted grids and P_e is the proportion of grids consistently predicted by the simulation in the random state. When the kappa coefficient is $\geq$0.75, the simulation accuracy is higher. When 0.4 $\leq$ kappa coefficient < 0.75, the simulation accuracy is normal. When the kappa coefficient is < 0.4, the simulation accuracy is low.

3. Results and Discussion

3.1. Temporal and Spatial Evolution Characteristics of Waterlogging Vulnerability in Fuzhou

3.1.1. Spatial Distribution Characteristics of Waterlogging Vulnerability in Fuzhou

By calculating the indicators' information entropy, the indicators' weights were calculated according to the discrete degree of the entropy value. The calculation results are shown in Table 3. Based on the weights of the indicators and the formula of the waterlogging vulnerability index, the vulnerability of Fuzhou to waterlogging in 2014, 2017, and 2020 was calculated. The vulnerability index was graded and finally divided into Level 1 vulnerable areas (−0.02–0.05), Level 2 vulnerable areas (0.05–0.12), Level 3 vulnerable areas (0.12–0.18), Level 4 vulnerable areas (0.18–0.28), and Level 5 vulnerable areas (0.28–0.62).

Table 3. Entropy method to calculate the weighting results.

Index	Weight	Index	Weight
Total annual rainfall	0.019	Normalized difference vegetation index	0.008
Number of annual rainstorms	0.009	Topographic wetness index	0.056
Annual storm peak	0.026	Topographic position index	0.002
Population density	0.29	Contagion index	0.032
Road network density	0.128	Shannon's diversity index	0.007
Building density	0.01	Education level	0.005
Night lighting	0.196	Medical level	0.006
Soil water retention	0.152	Disaster prevention and control capacity	0.013
Distance from the water system	0.002	Emergency evacuation distance	0.032
Slope	0.004	Drainage pipe network design standards	0.003

The spatial distribution characteristics of waterlogging vulnerability in Fuzhou are shown in Figure 3. The vulnerability to waterlogging in Fuzhou shows a "center-southeast" distribution pattern which is gradually decreasing. The central and southeastern regions are mainly of Level 4 and Level 5 vulnerability, while the Level 3 vulnerable areas are scattered around the water system of Fuzhou. The northwest and southwest regions are mainly of Level 1 and Level 2 vulnerability. As the Gulou, Taijiang, and Cangshan districts are the central urban areas specified in the overall urban plan of Fuzhou, the level of economic development and urbanization in these districts is high. Good economic conditions have led to high local population density and extensive road network construction, so that

disaster losses are greater when waterlogging is experienced. The southeast region is mainly Fuzhou's south-wing development zone, including the Fuqing central urban area, the Yuanhong investment zone, and the Jiangyin industrial concentration zone. These regions are characterized by highly concentrated industry and commerce; the economic losses caused by a waterlogging disaster are therefore higher in this region than in other regions affected by the same event; the vulnerability level in the southeast is therefore high. The northwestern part is mainly mountainous, with rich vegetation, high altitude, and a relatively low population, so that vulnerability to waterlogging in the southwestern part is lower. Zhang et al. [38] reported that increases in impervious surfaces and changes in natural water surfaces have had a large impact on waterlogging in Fuzhou.

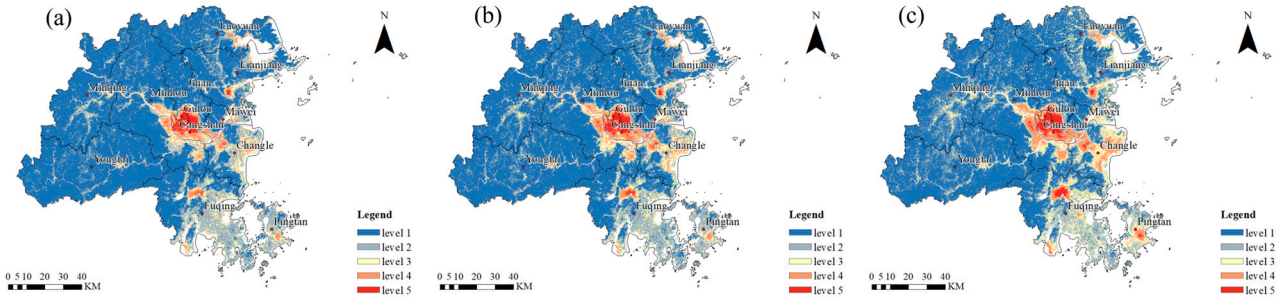

Figure 3. Assessment results of urban waterlogging vulnerability in Fuzhou: (**a**) 2014; (**b**) 2017; and (**c**) 2020.

3.1.2. Temporal Evolutionary Characteristics of Waterlogging Vulnerability in Fuzhou

The statistical analysis of the raster proportion of each level of vulnerability in Fuzhou is shown in Table 4. Between 2014 and 2017, the Level 1 and Level 2 areas in Fuzhou decreased by 177.6 km^2 (1.41%) and 16.8 km^2 (0.14%), respectively; the Level 3, Level 4 and Level 5 areas increased by 126 km^2 (1.05%), 44.4 km^2 (0.37%), and 26.4 km^2 (0.18%), respectively, with the most significant increase in Level 3 areas. Between 2017 and 2020, the vulnerability of the Fuzhou region to waterlogging increased significantly. In that time, the areas with vulnerability at Levels 2, 3, 4, and 5 increased by 284.4 km^2 (2.37%), 414 km^2 (4.45%), 103.2 km^2 (0.86%), and 39.6 km^2 (0.33%), respectively. In contrast, the area at Level 1 vulnerability decreased by 843.6 km^2 (7.03%) between 2017 and 2020.

Table 4. Extent of vulnerability-level areas in Fuzhou between 2014 and 2020.

Year	Level 1/km^2	Level 2/km^2	Level 3/km^2	Level 4/km^2	Level 5/km^2
2014	8518.8	1946.4	937.2	460.8	136.8
2017	8341.2	1929.6	1063.2	505.2	163.2
2020	7497.6	2214	1477.2	608.4	202.8

The spatial analysis function of ArcGIS was used to perform superposition analysis of the vulnerability assessment results for different periods, and a change-and-transfer matrix of vulnerability in the study area from 2014 to 2020 was obtained, as shown in Table 5. It was found that changes in waterlogging vulnerability in Fuzhou could be divided into five types: (1) Continuous-change types, such as the A–B–C type, mainly Level 1–Level 2–Level 3. (2) Repeated-change types, such as the A–B–A type, mainly Level 1–Level 2–Level 1 and Level 2–Level 1–Level 2. (3) Late-stage-change types, such as the A–A–B type, including changes from low-level to high-level and from high-level to low-level. (4) Early-stage-change types, such as the A–B–B type. This the type most evident in changes from Level 2 to other levels. (5) Stable types, such as A–A–A. Among these, The transformation area of the Level 1–Level 1–Level 1 change type was the highest, at 556.75 km^2. The transformation area of the Level 5–Level 5–Level 5 change type was lowest, at only 9.18 km^2. The stable area accounted for 74.91%, which can be understood as an absolute dominant position. The

area that changed was mainly of the late-change type, accounting for 14.13%. Therefore, it can be considered that vulnerability to waterlogging in most areas of Fuzhou changed between 2017 and 2020.

Table 5. Different types of change in waterlogging vulnerability in Fuzhou from 2014 to 2020.

Type	Main Types of Change	Area/km^2	Scale/%
Stable	Level 1–Level 1–Level 1	556.75	62.5
	Level 2–Level 2–Level 2	58.53	6.57
	Level 3–Level 3–Level 3	26.28	2.95
	Level 4–Level 4–Level 4	16.57	1.86
	Level 5–Level 5–Level 5	9.18	1.03
Early-stage change	Level 1–Level 2–Level 2	17.55	1.97
	Level 2–Level 1–Level 1	9.89	1.11
	Level 2–Level 3–Level 3	16.12	1.81
	Level 3–Level 2–Level 2	5.88	0.66
	Level 3–Level 4–Level 4	6.95	0.78
Late-stage change	Level 1–Level 1–Level 2	62.89	7.06
	Level 1–Level 1–Level 3	7.39	0.83
	Level 2–Level 2–Level 1	5.7	0.64
	Level 2–Level 2–Level 3	33.76	3.79
	Level 3–Level 3–Level 2	4.81	0.54
	Level 3–Level 3–Level 4	11.31	1.27
Repeated change	Level 1–Level 2–Level 1	10.42	1.17
	Level 2–Level 1–Level 2	10.33	1.16
	Level 2–Level 3–Level 2	6.68	0.75
	Level 3–Level 2–Level 3	8.28	0.93
Continuous change	Level 1–Level 2–Level 3	5.61	0.63

To further understand the characteristics of the changes in the vulnerability of Fuzhou, the types with a relatively large transformation area from 2014 to 2020 were screened and visualized, and changes in the vulnerability index of Fuzhou calculated, as shown in Figure 4. It can be seen that the transformation area is concentrated in the eastern coastal area and is characterized by mainly high vulnerability levels, while the vulnerability of the western area is mainly at Levels 1 and 2. These areas are mainly located in the urban area of Fuzhou close to the Minjiang River; according to the current trend, these areas are most likely to be transformed to Level 5 vulnerability in the future. Therefore, we need to focus on these areas when planning future disaster prevention and mitigation. The areas with greatest increases in their vulnerability index are mainly distributed in Fuqing City, Pingtan County, and Minhou County; of these, Fuqing City has experienced the greatest increase in its vulnerability index. The main reason is that Fuqing City has gradually improved its road network by means of intensified road construction in recent years. Changfu Expressway and the Binhai transport corridor were both constructed during this period, and the original national, provincial, and county roads were upgraded and reconstructed. The road network is now denser than it was in 2014, and this has driven the development of industry, the aggregation of population, and the promotion of economic development. However, the corresponding urban drainage facilities have not kept up with the construction, resulting in a sharp rise in the vulnerability index of the region. In the Level 5 vulnerable areas, which are mainly in the center of the study region, the vulnerability level has not changed, but the corresponding vulnerability index has decreased. This shows that the corresponding disaster reduction measures are effective and can reduce the vulnerability of urban waterlogging.

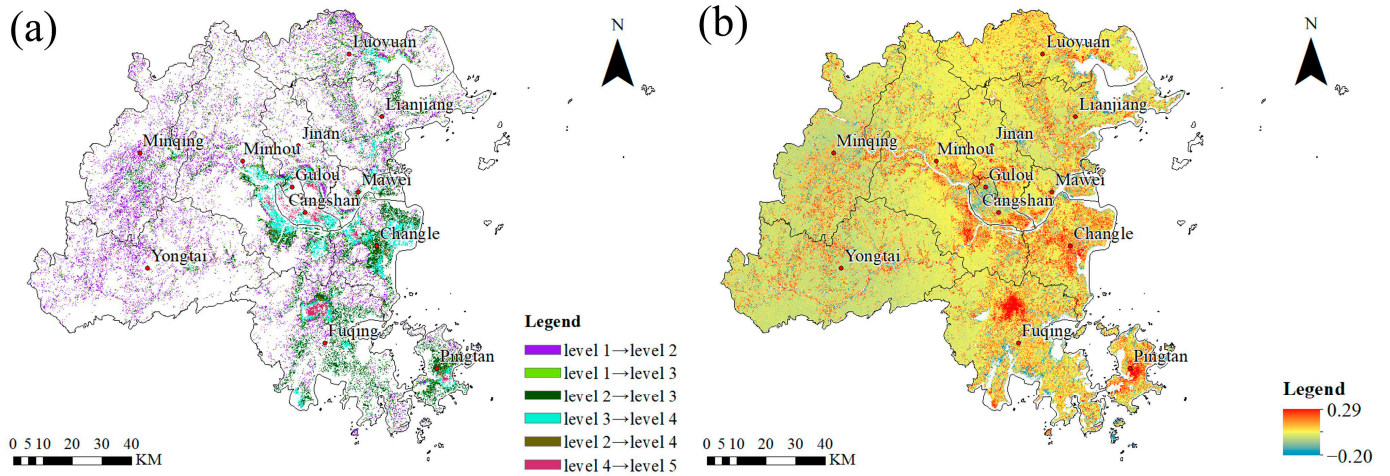

Figure 4. Characteristics of temporal evolution of waterlogging vulnerability in Fuzhou from 2014 to 2020: (**a**) main vulnerability transformation types in Fuzhou; (**b**) change amplitude of vulnerability index in Fuzhou.

3.2. Future Prediction of Waterlogging Vulnerability in Fuzhou

3.2.1. CA–Markov Simulation Accuracy Check

The CA–Markov model was used to simulate the waterlogging vulnerability of Fuzhou in 2020 using the results of the waterlogging vulnerability assessments in 2014 and 2017 as the base data. The simulation result and the actual situation are shown in Figure 5. It can be seen that their spatial distribution characteristics are consistent. The average error of the simulation result for 2020 is 8.44% for each vulnerability level, relative to the actual results which are shown in Table 6. Among these results, the simulation error for Level 3 vulnerability is the highest, at −19.82%, and the simulation error for Level 2 vulnerability is the lowest, at −3.79%. The kappa coefficient of the predicted waterlogging vulnerability in Fuzhou in 2020 is 0.9079, indicating that the model is feasible and applicable to the prediction of waterlogging vulnerability in Fuzhou.

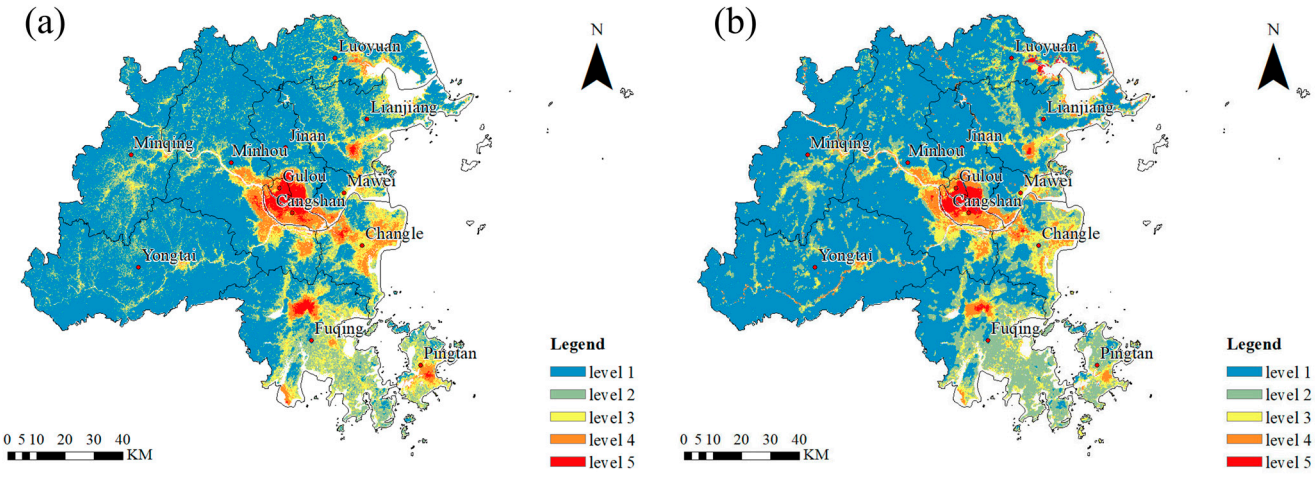

Figure 5. Accuracy check of Fuzhou waterlogging vulnerability prediction: (**a**) real waterlogging vulnerability in Fuzhou in 2020; (**b**) forecast waterlogging vulnerability in Fuzhou in 2020.

Table 6. Area proportions and relative errors between the simulation result and the actual situation for each vulnerable level in Fuzhou in 2020.

Waterlogging Vulnerability Level	Simulated Area Ratio/%	Actual Area Ratio/%	Relative Error/%
Level 1	66.07	62.48	5.75
Level 2	17.75	18.45	−3.79
Level 3	9.87	12.31	−19.82
Level 4	4.72	5.07	−6.9
Level 5	1.59	1.69	−5.92

3.2.2. Results of Predictions of Future Waterlogging Vulnerability in Fuzhou

Based on the vulnerability assessment results for Fuzhou in 2017 and 2020, the CA—Markov model was used to predict the vulnerability of Fuzhou City to internal waterlogging in 2023, 2026, and 2029. The simulation results are shown in Figure 6. It can be seen that the regions with the largest predicted change in vulnerability in Fuzhou between 2020 to 2029 are concentrated on the eastern coast; this is consistent with the changing trend of vulnerability in Fuzhou from 2013 to 2020. The vulnerability levels of Luoyuan County and Lianjiang County in the northeast exhibit the greatest change, generally from Levels 3 and 4 to Level 5. In the eastern Changle District and in the southeastern Pingtan County, vulnerability levels are not predicted to increase but instead exhibit a trend of spreading into surrounding areas.

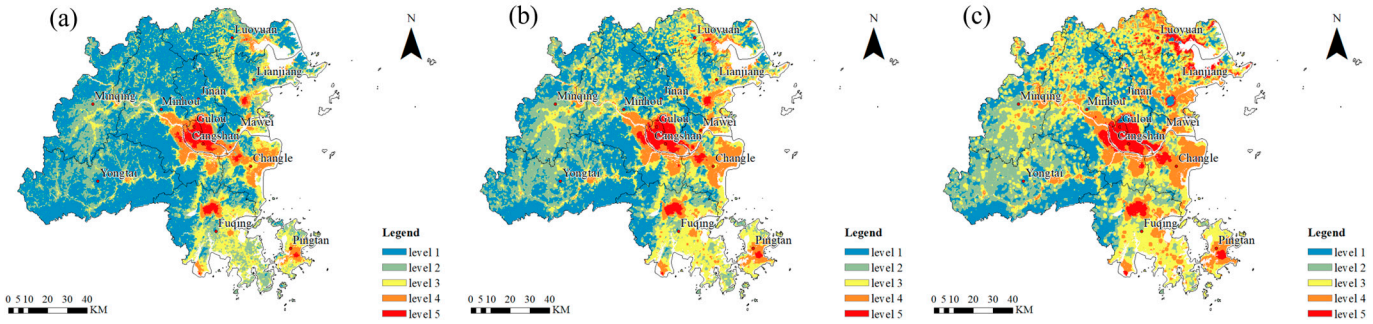

Figure 6. Forecasts of waterlogging vulnerability in Fuzhou in: (**a**) 2023; (**b**) 2026 and (**c**) 2029.

The areas of waterlogging vulnerability levels in different years are shown in Table 7. Between 2020 and 2029, the extent of Level 1 vulnerable areas in Fuzhou is predicted to decrease by 3717 km^2, while Level 2, Level 3, Level 4, and Level 5 vulnerable areas are expected to increase in size by 459 km^2, 1646 km^2, 1115 km^2, and 494 km^2, respectively. Among them, the extent of Level 5 vulnerable areas is expected to grow faster and faster with the passage of time. In summary, the extent of the areas in Fuzhou which are vulnerable to waterlogging is increasing with time, and the vulnerability level continues to deteriorate. Therefore, it is necessary to strengthen further the optimization and control of vulnerable areas in Fuzhou.

Table 7. Predicted extent of vulnerable level areas in Fuzhou between 2023 and 2029.

Year	Level 1/km^2	Level 2/km^2	Level 3/km^2	Level 4/km^2	Level 5/km^2
2023	5853.5	3068.6	1975.9	824.6	246.5
2026	3896.8	3707.7	2775.4	1235.1	353.1
2029	2136.3	3528.2	3622.7	1940.0	740.8

4. Conclusions

In this study, taking Fuzhou as the research object, we constructed a waterlogging vulnerability assessment system, calculated a waterlogging vulnerability index for the

period from 2014 to 2020, and predicted future trends in vulnerability. The main conclusions drawn may be stated as follows:

(1) The vulnerability of waterlogging in Fuzhou is characterized by a gradually decreasing "center-southeast" distribution pattern. Level 1 and Level 2 vulnerable areas are distributed in Fuzhou's northwestern and southwestern areas. In contrast, Level 3 vulnerable areas are scattered around the water system of Fuzhou. Level 4 and Level 5 vulnerable areas are concentrated in central areas such as Gulou District, Taijiang District, Cangshan District, and the southeastern development area of the south wing of Fuzhou.

(2) Between 2014 and 2017, and between 2017 and 2020, Level 1 regions exhibited the greatest decreases in vulnerability, of 1.41% and 7.03%, respectively. Level 3 regions showed the largest increases, of 1.05% and 4.45%, respectively. The change in the vulnerability of Fuzhou to waterlogging between 2014 and 2020 can be divided into five change modes, in which the change of regional types is mainly in the later stage. The change of region types was concentrated in the eastern coastal area, and was characterized mainly by transition between high vulnerability levels. The areas with the highest increases in their vulnerability index were Fuqing County, Pingtan County, and Minhou County, largely because of the construction of new road networks in these areas. In future disaster prevention and mitigation, focusing on areas with rapid road network construction is necessary.

(3) The CA–Markov model can accurately predict waterlogging vulnerability with a kappa coefficient of 0.9079. Between 2020 and 2029, the vulnerability of Fuzhou is expected to increase further. In the counties of Luoyuan and Lianjiang in the northeast, the regional vulnerability level is predicted to rise generally to Level 5, while in Changle district in the east, and in Pingtan County in the southeast, the regional vulnerability level is mainly predicted to exhibit a trend of spreading to surrounding areas. With the passage of time, the proportion of Level 5 vulnerable areas is expected to increase faster and faster.

(4) This study has a limitation with respect to the modeling of waterlogging vulnerability at Level 3. It can be seen that the error reaches −19.82% in this case. However, in this study, we have improved the model accuracy for Fuzhou to the greatest degree possible using existing technology and data, and although the error is large for the simulation of Level 3, the methods described in paper nevertheless represent a new means of applying the CA–Markov model for the prediction of waterlogging vulnerability levels.

Author Contributions: X.W., Z.Z. and W.H. contributed to the conceptualization, data analysis, and visualization of the study. X.W. and W.H. contributed to the writing of the paper. X.Z., X.Q. and R.C. contributed to the revision of the paper. All authors have read and agreed to the published version of the manuscript.

Funding: Please add: This research was funded by the National Key R&D Program of China (Grand No. 2022YFC3800500).

Data Availability Statement: Please contact the corresponding author for data.

Conflicts of Interest: Author Ran Cai was employed by the company Beijing Capital Ecological Protection Group. The remaining authors declare that the research was conducted in the absence of any commercial or financial relationships that could be construed as a potential conflict of interest.

References

1. Hu, W.; Zhang, Z.; Zhao, X.; Qi, X.; Wang, Y. VSD model and geodetector-based assessment on urban waterlogging vulnerability in Beijing and analysis of its driving mechanism. *Water Resour. Hydropower Eng.* **2022**, *53*, 86–100.
2. Zachos, L.G.; Swann, C.T.; Altinakar, M.S.; Mcgrath, M.Z.; Thomas, D. Flood vulnerability indices and emergency management planning in the Yazoo Basin, Mississippi. *Int. J. Disaster Risk Reduct.* **2016**, *18*, 89–99. [CrossRef]
3. Solín, L.; Madajová, M.S.; Michaleje, L. Vulnerability assessment of households and its possible reflection in flood risk management: The case of the upper Myjava basin, Slovakia. *Int. J. Disaster Risk Reduct.* **2018**, *28*, 640–652. [CrossRef]
4. Papathoma-Köhle, M.; Schlögl, M.; Dosser, L.; Roesch, F.; Borga, M.; Erlicher, M.; Keiler, M.; Fuchs, S. Physical vulnerability to dynamic flooding: Vulnerability curves and vulnerability indices. *J. Hydrol.* **2022**, *607*, 127501. [CrossRef]
5. Cummings, C.A.; Todhunter, P.E.; Rundquist, B.C. Using the Hazus-MH flood model to evaluate community relocation as a flood mitigation response to terminal lake flooding: The case of Minnewaukan, North Dakota, USA. *Appl. Geogr.* **2012**, *32*, 889–895. [CrossRef]

6. Remo, J.W.F.; Pinter, N.; Mahgoub, M. Assessing Illinois's flood vulnerability using Hazus-MH. *Nat. Hazards* **2015**, *81*, 265–287. [CrossRef]
7. Li, C.S.; Zhou, K.P.; Lin, Y. Vulnerability assessment of waterlogging disaster in old communities based on cloud matter-element. *J. Saf. Sci. Technol.* **2022**, *18*, 217–223.
8. Zheng, X.Z.; Wang, X.Y.; Zhou, S. Study on Vulnerability of Urban Waterlogging Disaster in Hubei Province. *Water Resour. Power* **2017**, *35*, 51–54.
9. Helderop, E.; Grubesic, T.H. Social, geomorphic, and climatic factors driving U.S. coastal city vulnerability to storm surge flooding. *Ocean Coast. Manag.* **2019**, *181*, 104902. [CrossRef]
10. Huang, H.; Li, H.; Zhang, Y.; Yang, X.; Chen, S. Construction of Urban Flooding Vulnerability Evaluation System and Vulnerability Assessment of Xi'an City Based on PSR and AHP Methods. *J. Nat. Disasters* **2019**, *28*, 167–175.
11. Christian, A.K.; Dovie, B.D.; Akpalu, W.; Codjoe, S.N.A. Households' socio-demographic characteristics, perceived and underestimated vulnerability to floods and related risk reduction in Ghana. *Urban Clim.* **2021**, *35*, 100759. [CrossRef]
12. Yao, R.; Yang, Q.T.; Zhang, S.L. Review on vulnerability of urban rainstorm waterlogging disaster. *Water Resour. Prot.* **2023**, *39*, 93–100.
13. Yierfanjiang, A.; Alimujiang, K.; Anwaer, M. Dynamic evolution and simulation prediction of urban vulnerability: Take Urumqi City as an example. *J. Glaciol. Geocrylogy* **2021**, *43*, 1861–1868.
14. Ait, E.H.F.; Ouadif, L.; Akhssas, A. Simulating and predicting future land-use/land cover trends using CA- Markov and LCM models. *Case Stud. Chem. Environ. Eng.* **2023**, *7*, 100342.
15. Aniah, P.; Bawakyillenuo, S.; Codjoe, S.N.A.; Dzanku, F.M. Land use and land cover change detection and prediction based on CA-Markov chain in the savannah ecological zone of Ghana. *Environ. Chall.* **2023**, *10*, 100664. [CrossRef]
16. Yao, K.; Zhang, C.; He, L.; Li, Y.; Li, X. Dynamic evaluation and prediction of ecological environment vulnerability in the middle—upper reaches of the Yalong River. *Remote Sens. Land Resour.* **2020**, *32*, 199–208.
17. Mokarram, M.; Pourghasemi, H.R.; Hu, M.; Zhang, H. Determining and forecasting drought susceptibility in southwestern Iran using multi-criteria decision-making (MCDM) coupled with CA-Markov model. *Sci. Total Environ.* **2021**, *781*, 146703. [CrossRef] [PubMed]
18. Polsky, C.; Neff, R.; Yarnal, B. Building comparable global change vulnerability assessments: The vulnerability scoping diagram. *Glob. Environ. Change* **2007**, *17*, 472–485. [CrossRef]
19. Li, C.; Li, J.; Zhang, M.; Zhang, D. Spatial and Temporal Distribution of Short-Lasting Heavy Rainfall in Beijing. *Meteorol. Sci. Technol.* **2015**, *43*, 704–708.
20. Wang, Y. Urban Stormwater Simulation and Waterlogging Risk Assessment Based on MIKE FLOOD. Master's Thesis, Hebei University of Engineering, Handan, China, 2018.
21. Ghosh, T.; LPowell, R.; DElvidge, C.; EBaugh, K.; CSutton, P.; Anderson, S. Shedding Light on the Global Distribution of Economic Activity. *Open Geogr. J.* **2010**, *3*, 147–160.
22. Chen, J.L.; Chen, W.J.; Huang, G.R. Urban Waterlogging Risk Assessment Based on Scenario Simulation and Multi-source Data. *Water Resour. Power* **2021**, *39*, 55–59.
23. Qi, X.; Zhang, Z. Assessing the urban road waterlogging risk to propose relative mitigation measures. *Sci. Total Environ.* **2022**, *849*, 157691. [CrossRef]
24. Tian, R.Y.; Wang, Y.K.; Fu, B.; Liu, Y. DEM-based topographic unit diversity index and its algorithm. *Prog. Geogr.* **2013**, *32*, 121–129.
25. Pourali, S.H.; Arrowsmith, C.; Chrisman, N.; Matkan, A.A.; Mitchell, D. Topography Wetness Index Application in Flood-Risk-Based Land Use Planning. *Appl. Spat. Anal. Policy* **2016**, *9*, 39–54. [CrossRef]
26. Zhao, W.D.; Gong, J.H.; Zhao, J.T.; Yang, W.T.; Gao, F. Research on topographic wetness index and its implications of surface water environment considering micro-reliefs on plains. *J. Hefei Univ. Technol. Nat. Sci.* **2019**, *42*, 113–118.
27. Roy, L.; Das, S. GIS-based landform and LULC classifications in the Sub-Himalayan Kaljani Basin: Special reference to 2016 Flood. *Egypt. J. Remote Sens. Space Sci.* **2021**, *24*, 755–767. [CrossRef]
28. Wu, J.S.; Zhang, P.H. The effect of urban landscape pattern on urban waterlogging. *Acta Geogr. Sin.* **2017**, *72*, 444–456.
29. Pham, B.T.; Luu, C.; Van Dao, D.; Van Phong, T.; Nguyen, H.D.; Van Le, H.; von Meding, J.; Prakash, I. Flood risk assessment using deep learning integrated with multi-criteria decision analysis. *Knowl.-Based Syst.* **2021**, *219*, 106899. [CrossRef]
30. Li, H.; Zhao, X.Y.; Wang, W.J.; Li, W. Inherent Vulnerability of Rural Society in Gannan Plateau, China and Its Influencing Factors. *Sci. Geogr. Sin.* **2020**, *40*, 804–813.
31. Cai, X.; Li, Z.; Zhang, H.; Xu, C. Vulnerability of glacier change in Chinese Tianshan Mountains. *Acta Geogr. Sin.* **2021**, *76*, 2253–2268.
32. *GB50014–2021*; Ministry of Housing and Urban Rural Development of the People's Republic of China. Standard for Design of Outdoor Wastewater Engineering. China Planning Press: Beijing, China, 2021.
33. Saha, T.K.; Pal, S.; Sarkar, R. Prediction of wetland area and depth using linear regression model and artificial neural network based cellular automata. *Ecol. Inform.* **2021**, *62*, 101272. [CrossRef]
34. Wang, Y.; Chen, F.; Wei, F.; Yang, M.; Gu, X.; Sun, Q.; Wang, X. Spatial and temporal characteristics and evolutionary prediction of urban health development efficiency in China: Based on super-efficiency SBM model and spatial Markov chain model. *Ecol. Indic.* **2023**, *147*, 109985. [CrossRef]

35. Liu, X.; Ju, Q.; Ju, X.; Sun, Y.; Lian, Z.; Fu, X. Simulation and prediction of land use change in the middle and lower reaches of the Wei River based on CA-Markov model. *Water Sav. Irrig.* **2022**, *8*, 1–8.
36. Ru, S.F.; Ma, R.H. Ecological vulnerability assessment, spatial analysis and prediction of the Yellow River Basin. *J. Nat. Resour.* **2022**, *37*, 1722–1734.
37. Wang, L.; Zhang, J.; Meng, N.; Sui, L.; Zhang, S.; Liu, Z. Simulation and prediction of temporal and spatial changes of NDVI in the Weihe River Basin based on CA-Markov. *Res. Soil Water Conserv.* **2020**, *27*, 206–212.
38. Zhang, J.; Wang, X.; Hou, Y.; Cai, L. A study of the impact of urbanisation progress on waterlogging in Fuzhou. *J. Catastrophology* **2018**, *33*, 146–151.